

RECTIFICATION OF THE DIURNAL CYCLE OVER SMALL ISLANDS IN RADIATIVE-CONVECTIVE EQUILIBRIUM

Timothy W. Cronin* and Kerry A. Emanuel

Program in Atmospheres, Oceans, and Climate, Massachusetts Institute of Technology, Cambridge, MA

1. INTRODUCTION

Convective heating over the Maritime Continent (MC) plays a major role in the atmospheric general circulation, but is poorly represented in general by global models, which often suffer a dry bias over the region (Neale and Slingo 2003). Recent observations that precipitation is greater over islands as compared to the surrounding ocean regions (e.g. Sobel et al. (2011)), together with the strong observed diurnal cycle in precipitation (e.g. Yang and Slingo (2001)), have led to hypotheses that the diurnal cycle may be related to the enhancement of time-mean precipitation over islands (Neale and Slingo 2003; Qian 2008; Robinson et al. 2008). However, the mechanisms responsible for such "rectification" of the diurnal cycle remain somewhat unclear, and the hypotheses of different authors are somewhat divergent. A common thread in all three of these studies, as well as other work on modeling of precipitation over tropical islands (Sato et al. 2009; Robinson et al. 2011), is invocation of the importance of dynamical convective forcing due to low-level convergence of land-sea and mountain-valley breezes. However, the complexity of such circulations in real terrain, especially in concert with other differences between the land and ocean lower boundaries, makes it difficult to precisely identify whether or not such forcing is a primary or essential mechanism of rectification. Here, we attempt to ask a somewhat more basic question by throwing away all land-ocean contrasts except the difference in heat capacity. We thus pose the question of whether the lower heat capacity of an island, by itself, can induce rectification of the diurnal cycle and precipitation enhancement over an island compared to the surrounding ocean.

In this study, we present results from idealized simulations of radiative-convective equilibrium in a cloud-system-resolving model, where a "swamp island" of shallow slab-ocean is embedded in a larger region of deeper slab-ocean. For a low-heat capacity island 96 km by 96 km in size, long-term average precipitation

is more than doubled over the island relative to the ocean-average, with strong time-mean ascent in the mid- and upper- troposphere over the island largely compensated by a dry ring of subsidence over the nearby ocean. We identify two radiative mechanisms that result in an atmospheric energy surplus over the island, thus providing forcing for time-mean ascent and precipitation enhancement. One is a clear-sky mechanism, resulting principally from the nonlinearity of surface enthalpy fluxes with respect to the surface temperature disequilibrium (Randall et al. 1991). The other is a cloudy-sky mechanism, resulting from both a shortwave component – the lagged phase relation between solar radiation and cloudiness over the island causes anomalously low reflected solar radiation – and a longwave component – greater mean cloudiness over the island causes anomalously low OLR. While the longwave component is probably better thought of as a feedback than a forcing, both components give rise to strongly positive net cloud radiative effect over the island and nearby ocean.

2. METHODS

The core goal of this study is to examine the mechanisms by which the interaction of the diurnal cycle of solar radiation solely with the differential heat capacities of land and ocean surfaces can rectify into time-mean differences between the land and ocean. To this end, we perform simulations of statistical radiative-convective equilibrium (RCE) with version 6.8.2 of the System for Atmospheric Modeling (SAM, Khairoutdinov and Randall (2003)) cloud-system-resolving model. In all of our experiments, the domain is doubly-periodic, 384 by 384 km with 3-km horizontal resolution and a stretched grid with 64 levels in the vertical. Such resolution is relatively coarse, but as we have in mind both significantly larger domains, and runtimes of hundreds of days, relatively coarse resolution is necessary for the majority of simulations. In all of our simulations, dynamics are non-rotating, there is no background flow, and we use CAM radiation and SAM 1-moment mi-

*Corresponding author address: Timothy W. Cronin, Massachusetts Institute of Technology 54-1717, Cambridge, MA 02139; email: twcronin@mit.edu

crophysics. Surface temperatures are interactive everywhere – that is to say the model explicitly solves a prognostic equation for slab surface temperature T_s in each grid cell:

$$C_s \frac{\partial T_s}{\partial t} = R_n - H - E, \quad (1)$$

where R_n is the net radiation at the surface (short-wave plus longwave, positive downwards), H is the surface sensible heat flux, and E is the surface latent heat flux (turbulent fluxes positive upwards). The surface heat capacity C_s is the sole difference between land and ocean, and is set to $4 \times 10^6 \text{ J m}^{-2} \text{ K}^{-1}$ for “ocean” grids ($\sim 1 \text{ m}$ water), and $2 \times 10^5 \text{ J m}^{-2} \text{ K}^{-1}$ for “land” or “island” grids ($\sim 5 \text{ cm}$ water). Quotes are included here to emphasize that the surfaces are extremely idealized, but we will drop the quotations hereafter.

The choices of C_s for land and ocean were driven by the twin goals of minimizing simulation times, and ensuring stability of the land surface temperature equation. This leads to a relatively low value of ocean C_s , and a relatively high value of land C_s – the factor of 20 difference between the two is quite a bit smaller than is realistic, but is nonetheless sufficient to drive a diurnal cycle of T_s with peak-to-trough amplitude $\sim 30 \text{ K}$ over land but only $\sim 2 \text{ K}$ over the ocean (diurnal composites of surface temperature from a simulation with both surfaces are shown in Figure 3). Future simulations will examine the dependence of results on the choice of C_s . It is worth noting that RCE with interactive T_s has substantially longer equilibration timescales than RCE with fixed T_s (e.g. fixed-SST), even as the surface heat capacity becomes small. The e -folding equilibration time in the simulations presented here ranges from ~ 60 to ~ 120 days or so. This is several times longer than the typical “long” fixed-SST RCE (e -folding) adjustment timescale of ~ 20 days (e.g. Tompkins and Craig (1998)). Use of fixed T_s for a climate-scale problem is generally inadvisable in that it immediately discards energy balance, which is one of the core principles underlying our understanding of climate. Thus, simulations with interactive T_s are much more computationally expensive, but necessary in our view, both to preserve energy balance, and to reasonably simulate a land surface.

Our longer equilibration timescales (as compared to typical fixed-SST RCE studies) are a direct result of the fact that RCE with interactive T_s is an energetically open system across only the top boundary, while RCE with fixed T_s is an energetically open

system across both the top and bottom boundaries. Since the sensitivity of surface energy fluxes to a perturbation in surface air temperature is much stronger than the sensitivity of top-of-atmosphere (TOA) net radiation to a perturbation in column temperature, a fixed- T_s simulation that starts too cold will rapidly gain most of its heat through the surface, while an interactive- T_s simulation that starts too cold must slowly gain all of its heat through the TOA. We can form timescale estimates in the two cases and show that they diverge even as C_s goes to zero. We expect that the equilibration timescale with interactive surface temperature (τ_{INT}) should scale as:

$$\tau_{\text{INT}} \sim (C_a + C_s) \left(\frac{\partial R_{\text{TOA}}}{\partial T_a} \right)^{-1}, \quad (2)$$

where R_{TOA} is the net top-of-atmosphere radiation (W m^{-2}), C_a is the column-integrated change in atmospheric moist static energy per unit area per Kelvin ($\text{J m}^{-2} \text{ K}^{-1}$), and T_a is the surface air temperature. This equation reflects the fact that the only way for the column to lose or gain energy and come to equilibrium is through the top-of-atmosphere. Note that the derivative $\frac{\partial R_{\text{TOA}}}{\partial T_a}$ is equivalent to the inverse of the climate sensitivity (temperature change per unit energy flux change). If the sea surface temperature is held fixed, then the timescale (τ_{FIX}) changes significantly:

$$\tau_{\text{FIX}} \sim C_a \left(\frac{\partial R_{\text{TOA}}}{\partial T_a} + \frac{\partial R_n}{\partial T_a} - \frac{\partial H}{\partial T_a} - \frac{\partial E}{\partial T_a} \right)^{-1}. \quad (3)$$

The conventional explanation for longer timescales with interactive surface temperature is that the long timescales are introduced by the large thermal inertia of an ocean surface ($C_s \gg C_a$ in (2) for typical mixed-layer ocean depths). However, if we set $C_s=0$ in (2), there can still be a notable difference in timescales τ_{INT} and τ_{FIX} ($C_s \ll C_a$ is in fact appropriate for a land surface). Longer timescales emerge simply because all the terms in parentheses in (3) are positive (net radiation out of the bottom of the atmosphere increases with increasing surface air temperature, turbulent surface fluxes decrease with increasing air temperature), and as noted above, these energetic coupling terms are large relative to the top-of-atmosphere energetic coupling. We can thus obtain a much shorter timescale simply because we are dividing by a much larger number in (3) than in (2), rather than due to any intrinsic difference in the thermal inertia of the system.

The solar insolation is a key aspect of the model

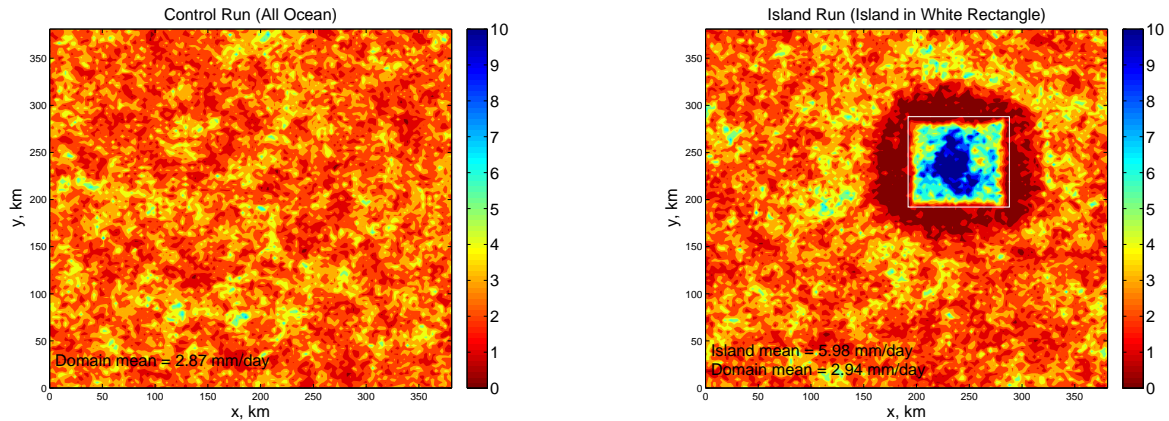


Figure 1: Time-mean precipitation in mm/day, for last 40 days of 250-day model simulations for control run (left) and island run (right). The location of the island is outlined with a white rectangle, and the domain-mean precipitation rates are noted in black text on the subfigures, as well as the island-mean precipitation rate.

setup, and determines the mean temperature that results from model simulations. Through trial-and-error, we have used a solar insolation corresponding to that at 45° N on the spring equinox (day of year 80), resulting in a TOA insolation of 310.3 W m^{-2} . This is obviously a much smaller value of the time-mean insolation than occurs for real tropical locations ($\sim 420 \text{ W m}^{-2}$), but a lower energy input to the system is necessary in order to avoid the runaway greenhouse regime. The alternate approach of prescribing a surface energy sink and using realistic tropical insolation is taken by Romps (2011), but it makes little sense to prescribe a surface energy sink over land.

We discuss the results from four different simulations here. The first is the “control” simulation with an all-ocean lower boundary. The second is the “island” simulation, which has a 96 by 96 km square island embedded in the domain. The third is the “lake” simulation, where land and ocean are inverted from the “island” run – so there is a lake embedded in a land domain. The fourth simulation has an identical lower boundary to the “island” run, but the radiation code always uses a cloud water and ice path of zero – thus we call this the “no-cloud-optics island” simulation. In Section 3, we briefly discuss the results of the control and island simulations, then we discuss in some detail two radiative mechanisms consistent with our results. In Section 4, we discuss some additional simulations and their implications for the interpretation of our work. In Section 5, we summarize our findings and suggest avenues for future work.

3. RESULTS: CONTROL AND ISLAND RUNS

Comparison of the time-mean precipitation in the control and island simulations reveals that the island has a dramatic impact on the spatial distribution of precipitation within the domain (Figure 1). In the island run, the time-mean precipitation over the island – 5.98 mm/day – is more than double the time-mean precipitation averaged over the whole domain – 2.94 mm/day . There is a clear dry ring around the island, which actually extends a small number of grid cells in from the coast. One question that we should ask is whether the island is simply “stealing” rainfall from this nearby ring of ocean, or whether the island also has an impact on the domain-averaged precipitation rate. The answer is mostly the former – moisture converged by the sea breeze rains out over the island and robs the nearby ocean of water vapor that could have rained over the ocean.

The impacts of the island on the domain-averaged temperature and precipitation are small but significant. The time- and spatially-averaged precipitation rate is $2.87 \pm 0.02 \text{ mm/day}$ in the control run and $2.94 \pm 0.02 \text{ mm/day}$ in the island run – and so the island leads to a small domain-mean precipitation enhancement of $2 \pm 1\%$ relative to the control run (error estimates here and elsewhere represent \pm two standard errors of the mean, based on hourly data at each grid point from the last 40 days of 250-day simulations). Time- and spatially-averaged air temperature differences have a great deal of structure in the vertical, but are generally small in the lower troposphere and increase with height up to the tropopause. The island run is roughly 0.25 K warmer

than the control simulation at the lowest model level (40 m), and the maximum temperature difference grows with height to nearly 1.1 K at 12 km. Domain-mean warming will be discussed more in Section 4, in conjunction with the lake simulation results.

Why is there more rain over the island? And why is the domain as a whole warmer in the presence of the island? Below, we discuss two radiative mechanisms that result in an atmospheric energy surplus over the island, providing forcing for time-mean ascent and precipitation enhancement, and also leading to a domain-mean warming. The first is a clear-sky mechanism, and is linked to day-night asymmetries in the diurnal cycle of surface temperature over land. The second is a cloudy-sky mechanism, related to the phase relation between cloud cover and the diurnal cycle, and the mean cloud fraction. We will discuss each of these in some detail, and then discuss how they relate to the other simulations we have performed.

A. CLEAR-SKY MECHANISM

One notable effect of interactions between the island and the diurnal cycle is a marked reduction of clear-sky OLR over the island (Figure 2; the apparent blockiness of the figure is due to the fact that variables are averaged over 4x4 grid cell blocks in the radiative transfer code). The island clearly stands out from the nearby ocean, which has anomalously high OLR due to the fact that the subsiding air there is anomalously dry in the mid-troposphere. The island also stands out from the far-field ocean, so that the mean OLR over the island is 6 W m^{-2} lower than the mean OLR over the ocean. To first order, this can be explained by the fact that the time-mean island surface temperature is roughly 4 K colder than the time-mean ocean surface temperature – 291.7 K compared to 295.8 K (Figure 3). As a consequence, the island surface has less net longwave cooling than the ocean surface, and a bit over a quarter of this surface longwave cooling difference propagates through the atmospheric window and manifests as a difference in OLR at the top of the atmosphere. The difference in time-mean surface temperatures over the island and ocean is a direct response to the diurnal cycle and a strong day/night asymmetry in turbulent surface fluxes.

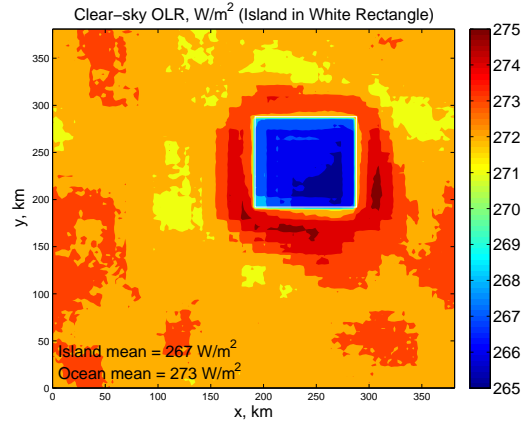


Figure 2: Time-mean outgoing longwave radiation (OLR, W m^{-2}) for last 40 days of 250-day model simulation for island run. The location of the island is outlined with a white rectangle, and the domain and island-mean OLR fluxes are noted in black text on the figure.

In these simulations, the key mechanism for producing this rectified response is the strongly nonlinear dependence of surface fluxes on the temperature disequilibrium between the surface and the air at the lowest model layer. This effect is described in some detail in section 5 of Randall et al. (1991), who found that including the diurnal cycle of insolation in a GCM reduced the time-mean land surface temperature by 2.7 K in the tropics, in spite of the fact that sea surface temperatures were fixed to the same climatological values in both simulations! Due primarily to the suppression of sensible and latent heat fluxes under stable conditions at night, the surface enthalpy flux depends nonlinearly, in a concave-up fashion, on the difference in temperature between the surface and surface air, $\Delta_{s-1} \equiv T_s - T_1$, where T_1 denotes the temperature of the lowest model layer. Downward enthalpy fluxes are nearly shut off at night when Δ_{s-1} is negative, but upward enthalpy fluxes are large during the day, when Δ_{s-1} is positive, and of a similar magnitude to nocturnal values. The nonlinearity of the Clausius-Clapeyron relation and the greater mean windspeed during the day both reinforce the basic mechanism invoked here, making surface fluxes more strongly nonlinear as a function of Δ_{s-1} . In order for surface energy balance to hold in the time-mean, with strongly nonlinear, concave-up enthalpy fluxes, the surface must be much colder than it would be in the absence of diurnal temperature variations.

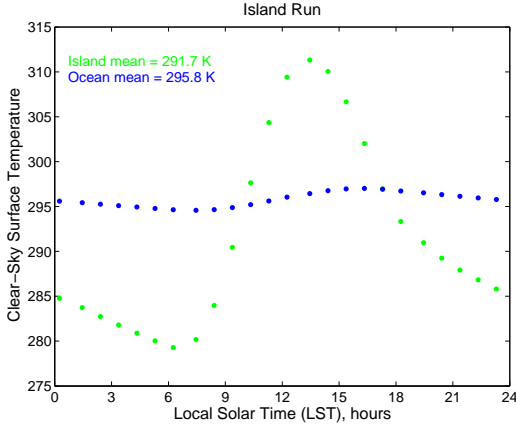


Figure 3: Diurnal composite of surface temperature for last 40 days of 250-day model simulation for island run. The time-mean island and ocean surface temperatures are indicated on the figure – the island surface is substantially colder than the ocean surface in the time-mean.

In this simulation, diurnal variations in the lowest model layer air temperature (T_1) over the island are small – only ~ 3 K – likely due to the smoothness of the surface, lack of background winds, and shallow boundary layer. The smooth surface and lack of background flow both give rise to a relatively weak coupling between the surface and lowest model layer, so in particular it is difficult to communicate cooling of the surface to even the lowest model level. In association with this weak coupling, the diurnal cycle of surface temperature is quite large – roughly 30 K – much larger than one might expect for a moist surface (e.g. a well-watered lawn). However, even the relatively small diurnal temperature range of T_1 exhibits rectification similar to that of T_s . The time-mean value of $T_{1,\text{island}}=291.4$ K is substantially lower than $T_{1,\text{ocean}}=292.5$ K. This can be thought of similarly to the surface temperature effect – in that the mechanism of cooling – convection – is a strongly nonlinear and concave-up function of the lower atmospheric stability (the time-mean of a fluctuating convective cooling $\overline{F(\theta_z(t))}$ driven by fluctuations of the stability $\theta_z(t)$ about a mean $\overline{\theta_z}$, is larger than the convective cooling driven by the time-mean stability $F(\overline{\theta_z})$; $\overline{F(\theta_z(t))} > F(\overline{\theta_z})$). When the lowest model layer is heated during the day, convective instability strongly limits the magnitude of warming that can occur, but when the lowest model layer is cooled, there is no similar limit on cooling. Rectification of the diurnal cycle of surface air temperature might become a more important factor in the column energy balance if the mean boundary layer were deeper, or if the surface and atmosphere were more strongly coupled, either by higher surface roughness or sub-

stantial mean winds. Interestingly, the impact of this diurnal rectification of T_1 is that there is a time-mean land breeze, which is confined to the boundary layer, and reinforced by the cold pool spreading associated with afternoon/evening convection over the island.

B. CLOUDY-SKY MECHANISM

Another notable effect of interactions between the island and the diurnal cycle is a strong positive cloud radiative effect (CRE) over both the island and the nearby “dry ring” of ocean (Figure 4). This mechanism is probably more important than the clear-sky mechanism discussed above, and also somewhat easier to think about, but it is unclear how much of it is truly a forcing and how much is a feedback to enhanced island convection that is initiated by, for instance, the clear-sky mechanism. Also, as it relies on cloud formation and lifetime, cloud-optics, and the timing of high clouds in the diurnal cycle, it may be more sensitive to model details and less robust than the clear-sky mechanism. The cloud radiative effect here is defined as the difference in TOA downward shortwave flux (SWCRE), TOA downward longwave flux (LWCRE), or their sum (CRE), for actual minus hypothetical-clear conditions. Hypothetical-clear conditions involve a parallel calculation in the radiative transfer code that sets the cloud water and ice path to zero; this calculation is purely diagnostic and does not affect the modeled radiative heating rates. In the control run, as over the background ocean in the island run, SWCRE (-) and LWCRE (+) are of similar magnitude and opposite sign, and balance to a net CRE of nearly zero.

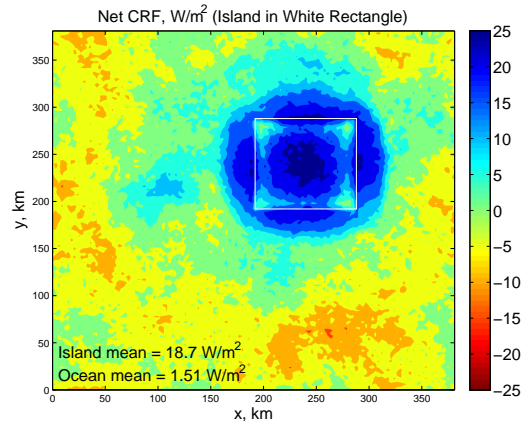


Figure 4: Net cloud radiative effect (CRE) – positive indicating net downward radiation – for last 40 days of 250-day model simulation for island run. The time-mean values are calculated over the island and the ocean and shown on the plot.

The positive CRE over the island and its vicinity shown in Figure 4 is a sum of shortwave and longwave cloud radiative effects (SWCRE, LWCRE) which differ from background ocean values in the same direction and with comparable magnitude (see Figure 6 for a decomposition of the net CRE into shortwave and longwave components). Reduction in negative SWCRE over the island (as compared to background ocean values) is related to the timing of clouds relative to the diurnal cycle of solar insolation. The peak of the cloud fraction occurs well after solar noon – it is in fact delayed until slightly after sunset (Figure 5). The shortwave CRE is -17.9 W m^{-2} over the island and -24.0 W m^{-2} over the ocean, so attributing the difference to the role of the diurnal cycle gives a diurnally driven ΔSWCRE of roughly 6 W m^{-2} . It is unclear to what extent these results are sensitive to the precise timing of this peak in the cloud fraction, and though it seems significant that the peak in cloud fraction occurs after sunset, this is probably not a requirement for a reduction in the magnitude of SWCRE compared to ocean values. However, it seems possible that the sign of the shortwave effect could change if the cloud-fraction distribution were shifted earlier by only a few hours. Enhanced LWCRE over the island occurs because there are simply more high clouds associated with the enhancement of deep convection. As mentioned above, this is likely better thought of as a feedback to other radiative and dynamical processes, rather than a mechanism which would exist on its own, such as the clear-sky effect. However, it is quite important, and the diurnally driven ΔLWCRE comes out to roughly 11 W m^{-2}

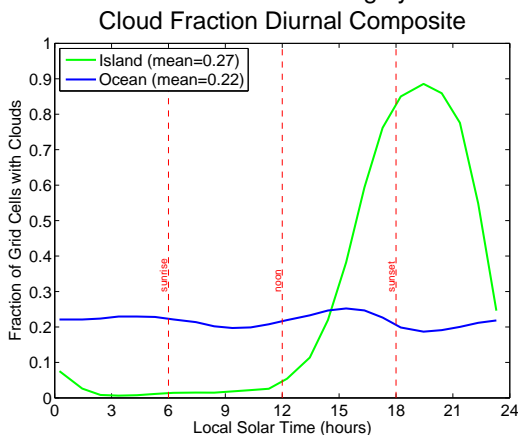


Figure 5: Diurnal composite of cloud fraction (fraction of grid cells with clouds) – for the last 40 days of 250-day model simulation for island run. The diurnal-mean values are calculated over the island and the ocean and shown on the plot, in the legend.

(36.6 W m^{-2} over the island as compared to 25.5 W m^{-2} over the ocean), or nearly double the shortwave effect.

The net CRE associated with the island also extends over a larger area than the island itself, due primarily to the suppression of clouds over the nearby ocean, and a consequent reduction of SWCRE (Figure 6). The positive LWCRE anomaly over the island is largely confined to the island itself, even though one might expect anvil cirrus to spread out beyond the spatial extent of the convectively active region (Figure 6). There is also a clear geometric structure to the total cloud radiative forcing on the scale of the island itself, with maxima near the center of the island and near the center of each of the four coastal edges, and pronounced minima near the four corners of the island. Visual inspection of the near-surface wind field (not shown), together with the SWCRE structure in Figure 6, suggests that the minima at the corners occur in association with sea-breeze convergence from two coasts, and cloud formation earlier in the day, resulting in a more strongly negative SWCRE. The center of the island represents a local maximum in SWCRE because substantial cloud cover does not arrive until the sea breeze does, in the mid-late afternoon, after most of the day’s sunshine has already occurred. Island size thus is naturally suggested as a variable that might play a strong role in controlling the phase lag between the peak insolation and peak cloud fraction, which is responsible for much of the spatial structure in total CRE in this simulation. Future simulations will explore use of a circular island, which should allow the importance of radius to be seen much more clearly.

4. RESULTS: NO-CLOUD AND LAKE RUNS

We have discussed two radiative mechanisms that arise as a consequence of the diurnal cycle over land in our simulations, and which we suggest play a significant role in both the enhancement of precipitation over the island, and the warming of the domain as a whole. Here, we discuss several other simulations that were conducted to explore the role of the radiative mechanisms, and preliminarily examine the importance of land fraction, geometry, and cloud radiative effects. One interesting result from the no-cloud optics island run (cloud liquid and ice water path always set to zero in radiative code) is that the clear-sky mechanism (perhaps along with some other unelucidated dynamical nonlinearity), results in a significant precipitation enhancement over an island without any cloud-radiation interactions (Figure

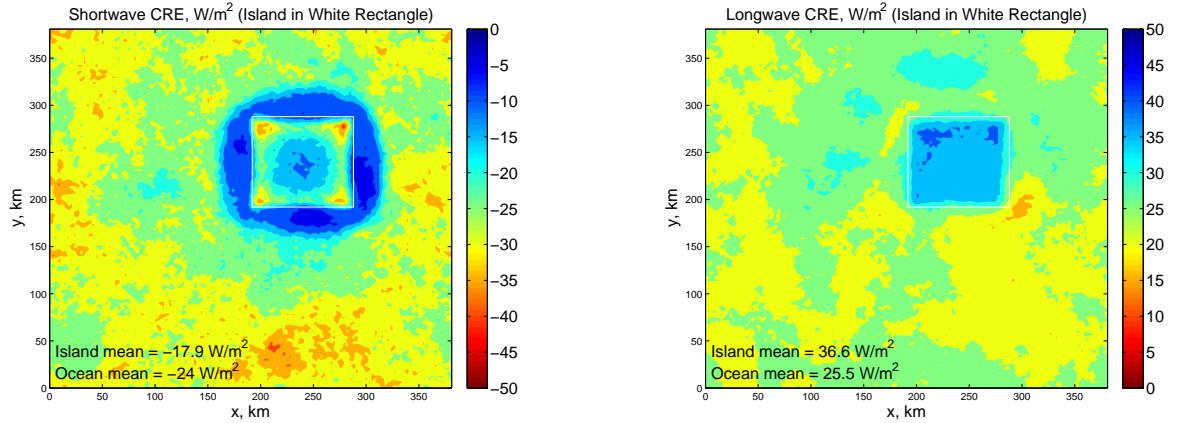


Figure 6: Breakdown of CRE into shortwave (SWCRE, left) and longwave (LWCRE, right) components – positive indicating net downward radiation – for last 40 days of 250-day model simulation for island run. The time-mean values are calculated over the island and the ocean and shown on the subplots. Note that the subplots have different scale ranges, since SWCRE is negative and LWCRE positive.

7). While the precipitation enhancement is greatly reduced as compared to the regular island run (58% as compared to 103%), the island still is much rainier than the surrounding ocean, and steals rainfall from a dry ring around it. It is not possible to do a direct comparison of the mean temperature or precipitation to other runs, though, because the absence of cloud radiative effects fundamentally alter some of the energetics of the system in RCE.

One major limitation of this study that we attempted to address with a different simulation is the importance of the sea breeze convergence in triggering

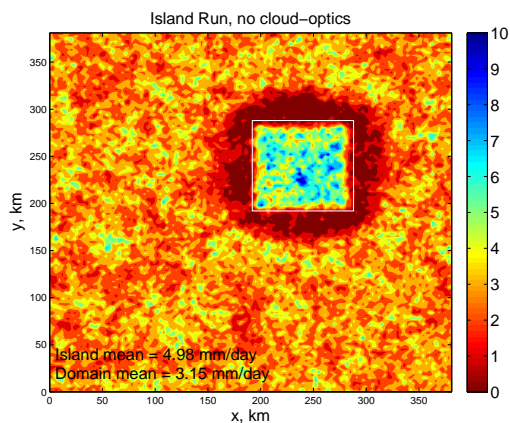


Figure 7: Time-mean precipitation for last 40 days of 250-day model simulations for island run with no cloud-optics (no SWCRE or LWCRE). The location of the island is outlined with a white rectangle, and the mean precipitation rates are noted in black text.

convection over the island, and/or in organizing convection over the island. As noted above, studies have often invoked the importance of sea breeze convergence in the formation of island thunderstorms, and it has been hypothesized as a mechanism which is important for the enhancement of precipitation over real islands. While the diurnally reversing land/sea breeze undoubtedly plays an important role in moisture and energy transport near the surface, it is not obvious what the rectification mechanism is for this circulation – e.g. why does the convergence associated with the sea breeze trigger convection, while the convergence associated with the land breeze does not? One asymmetry between these two patterns is that the sea-breeze convergence has a large magnitude over a small area, while the land-breeze convergence has a small magnitude over a large area. In an attempt to test whether this geometric asymmetry might explain much of the island precipitation enhancement, we performed a simulation where the island and ocean locations were inverted – a lake embedded in a region of land, rather than an island in an ocean. In this “lake run,” the lake turns out to be much drier than the domain as a whole, though there is a local maximum in precipitation near the center of the lake (Figure 8).

The radiative mechanisms discussed above both act to suppress precipitation over the lake, which has a larger clear-sky OLR, and a strongly negative CRF relative to the surrounding land – due to a very large negative SWCRF associated with the near-noon peak in cloud fraction, which dominates a positive LWCRF over the lake relative to the land.

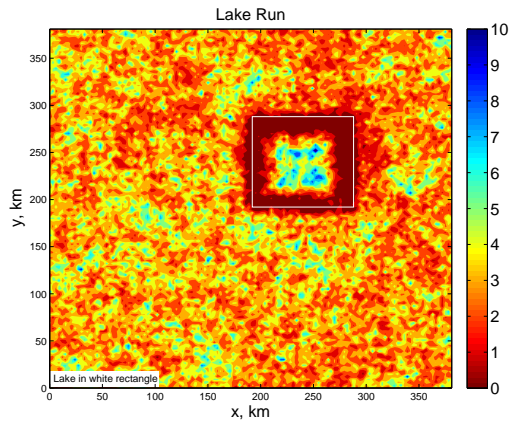


Figure 8: Time-mean precipitation for last 40 days of 250-day model simulations for lake run – the location of the lake is outlined with a white rectangle. Domain-mean precipitation is 3.35 mm/day, while the precipitation over the lake is only 2.17 mm/day.

A local precipitation maximum over the lake emerges, at least in part because the highly focused land breeze convergence provides strong forcing for lower-tropospheric ascent over the center of the lake. This simulation is in some ways quite similar to the island run, except that the dry ring of subsidence and nearly zero precipitation is inside the lake rather than outside the island. Circulations that result from island-ocean or land-lake contrasts must satisfy energy balance overall, which favors convection over land in light of the radiative mechanisms we have discussed, but due to the focused convergence over the minority terrain type, a local maximum of precipitation may also occur there.

The lake simulation also demonstrates a substantially warmer and rainier mean climate than the control run, due to the greater area over which the radiative mechanisms act (Figure 9; this is also true for an all-land simulation which will not be shown for brevity). Due to a shift in the timing of the cloud fraction peak over land, and the dispersed nature of the convection, the strength of the cloud radiative effect is weakened to near zero. This is an important result, and leaves the clear-sky mechanism as the dominant explanation of the warmer and moister conditions in the lake simulation as compared to the control or island runs. It also reiterates the key role of the phase lag between the solar forcing and cloud response, and points to the need for future simulations to better understand what controls it.

Domain-mean warming as the land fraction is increased can be thought of in terms of relaxation

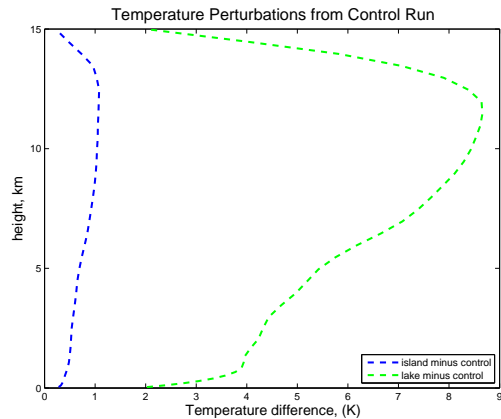


Figure 9: Time-mean differences in vertical profiles of domain-averaged temperature for island minus control (blue) and lake minus control (green) simulations. Comparisons are for last 40 days of 250-day model simulations.

towards strict convective quasiequilibrium (QE). Strict QE is never attained when the land fraction is substantial, but still represents a useful framework for thinking about the problem. Strict QE assumes that the free atmospheric temperature profile is convectively adjusted to a moist adiabat with saturation moist static energy that is equal to the moist static energy (MSE) at the top of the boundary layer. The diurnal cycle is too rapid for convection to reach strict QE with the boundary-layer maximum MSE that occurs each afternoon over land, but increasing the fraction of the domain that is covered by land allows the average convective activity over the domain to come closer to equilibrating with this afternoon BL MSE maximum. This diurnal maximum in BL MSE corresponds to a free-atmospheric moist adiabat that is considerably warmer than the moist adiabat corresponding to the time-mean BL MSE. Greater radiative cooling of the warmer free troposphere, as land fraction increases, is balanced by larger surface enthalpy fluxes, which are a result of surface energy balance and the lower surface radiative cooling implied by the clear-sky radiative mechanism.

5. CONCLUSIONS AND FUTURE WORK

We have presented results from several simulations of RCE with the SAM model, which show strong impacts of the diurnal cycle in the distribution of precipitation over a mixed ocean/land surface, simulated by varying the thickness of a wet slab surface. We have presented two radiative mechanisms by which the atmospheric column over an idealized moist land surface can obtain an energetic surplus, providing forcing for ascent and enhanced precipitation. The

clear-sky mechanism has been discussed before, but appears to not be widely recognized as important, though it may be able to drive domain-mean warming as well as land-localized precipitation enhancement. It may be possible to examine the robustness and realism of the clear-sky mechanism by looking in detail at observational datasets of land surface temperature.

One major uncertainty in the island simulation relates to the robustness of the phase lag between clouds and the diurnal cycle. This is a key uncertainty both because it regulates the strength of the cloud radiative effects here, and because it is known to be biased in GCMs – where convection and convective clouds peak near noon, or too early in the afternoon. We may be able to test the robustness of the phase lag by varying parameters in the model such as the land surface heat capacity, island size, and model resolution. Other key issues for future work include exploration of other surface properties that differ between real land and ocean surfaces, such as roughness, moistness, albedo, and elevation. Determining a method by which the column-radiative forcing and dynamical mechanisms such as convective triggering by land and sea breeze convergence can be compared on equal grounds will also be important for determining the importance of the radiative mechanisms discussed here relative to the oft-invoked role of dynamical forcing.

The finding that the domain-mean temperature increases with the addition of land suggests that extending this sort of simulation to the scale of an equatorial beta channel would result in mean ascent over areas with land, and compensating subsidence elsewhere. It remains to be seen whether this could result in circulations that look at all like the observed Walker circulation, or other tropical overturning circulations. Such a simulation could be accomplished by brute force – expanding the domain of a CRM simulation to the planetary scale. We will likely approach the problem with parameterized large-scale dynamics or by rescaling the equatorial deformation radius, by using a much larger value of β than occurs on the real Earth.

While this is obviously a highly idealized study and does not seek to reproduce the complexity of real land surfaces, which includes heterogeneous terrain and vegetation, we believe that idealized studies such as this are important for building understanding and clarifying the key mechanisms that govern real ocean-land-atmosphere interactions in the earth sys-

tem. This study suggests that the diurnal cycle may play an important role in the tropical precipitation distribution, merely by interacting with the heterogeneous heat capacity of land and ocean surfaces, and that the diurnal cycle may also impact tropical overturning circulations that play a key role in interannual variability of the climate.

6. ACKNOWLEDGMENTS

Thanks to Marat Khairoutdinov for supplying me with the model code, and to Allison Wing for teaching me how to use it. This work has been supported by NSF Grant 1136480, "The Effect of Near-Equatorial Islands on Climate," which is a collaboration with Peter Molnar.

7. REFERENCES

- Khairoutdinov, M. F. and D. A. Randall, 2003: Cloud Resolving Modeling of the ARM Summer 1997 IOP: Model Formulation, Results, Uncertainties, and Sensitivities. *Journal of the Atmospheric Sciences*, **60**, 607–625.
- Neale, R. B. and J. Slingo, 2003: The Maritime Continent and Its Role in the Global Climate : A GCM Study. *Journal of Climate*, **16**, 834–848.
- Qian, J.-H., 2008: Why Precipitation Is Mostly Concentrated over Islands in the Maritime Continent. *Journal of the Atmospheric Sciences*, **65** (4), 1428–1441.
- Randall, D. A., Harshvardhan, and D. A. Dazlich, 1991: Diurnal variability of the hydrologic cycle in a general circulation model. *J. Atmos. Sci.*, **48** (1), 40–62.
- Robinson, F. J., S. C. Sherwood, D. Gerstle, C. Liu, and D. J. Kirshbaum, 2011: Exploring the Land-Ocean Contrast in Convective Vigor Using Islands. *Journal of the Atmospheric Sciences*, **68** (3), 602–618.
- Robinson, F. J., S. C. Sherwood, and Y. Li, 2008: Resonant Response of Deep Convection to Surface Hot Spots. *Journal of the Atmospheric Sciences*, **65** (1), 276–286.
- Romps, D. M., 2011: Response of Tropical Precipitation to Global Warming. *Journal of the Atmospheric Sciences*, **68** (1), 123–138.
- Sato, T., H. Miura, M. Satoh, Y. N. Takayabu, and Y. Wang, 2009: Diurnal Cycle of Precipitation in

the Tropics Simulated in a Global Cloud-Resolving Model. *Journal of Climate*, **22 (18)**, 4809–4826.

Sobel, A. H., C. D. Burleyson, and S. E. Yuter, 2011: Rain on small tropical islands. *Journal of Geophysical Research*, **116 (D8)**, 1–15.

Tompkins, A. M. and G. C. Craig, 1998: Time-scales of adjustment to radiative-convective equilibrium in the tropical atmosphere. *Quarterly Journal of the Royal Meteorological Society*, **124**, 2693–2713.

Yang, G. and J. Slingo, 2001: The diurnal cycle in the tropics. *Monthly Weather Review*, **129**, 784–801.